Supporting information for the manuscript;

Melt-miscible oxalamide based nucleating agents and their nucleation efficiency in isotactic polypropylene

Yogesh S. Deshmukh[1], Carolus H. R. M. Wilsens[1,], Nils Leoné[1], Giuseppe Portale[2], Jules A.W. Harings[1], Sanjay Rastogi[1,]*.*

[1]Department of Biobased Materials, Faculty of Humanities and Sciences, Maastricht University, P.O. Box 616, 6200MD, Maastricht, The Netherlands. [2]Macromolecular Chemistry & New Polymeric Materials, Zernike Institute for Advanced Materials, Nijenborgh 4, 9747 AG, Groningen, The Netherlands.

*Corresponding authors: karel.wilsens@maastrichtuniversity.nl, sanjay.rastogi@maastrichtuniversity.nl

KEYWORDS: Nucleating agent, isotactic polypropylene, phase-diagram, shear-induced self-assembly.

Phase transitions and transition enthalpies of the NAs.

The peak values and their transition enthalpy observed in DSC analysis of the pure NA components, as is shown in Figure 3 of the manuscript, are summarized in Table S1 (heating run, Figure 3A) and Table S2 (cooling run, Figure 3B). T_1, T_2 reflect the transition temperatures of the crystal-to-crystal transitions occurring around 50 and 160 °C, respectively. The T_m and T_c denote the temperatures where the crystal-to-liquid and liquid-to-crystal phase transitions occur. Similarly, the ΔH_1, ΔH_2, ΔH_m, and ΔH_c denote the enthalpy involved in these transitions observed during heating and/or cooling.

Table S1. Phase transition observed in DSC analysis during the second heating run performed at 10 °C/min, including the enthalpy of the transitions.

	T_1 (°C)	ΔH_1 (J/g)	T_2 (°C)	ΔH_1 (J/g)	T_m (°C)	ΔH_m (J/g)
OXA 2,6	47	14.1	-	-	287	147.0
OXA 3,6	65	3.2	-	-	231	146.3
OXA 4,6	56	15.2	164	23.0	247	153.0

Table S2. Phase transition observed in DSC analysis during the second cooling run performed at 10 °C/min, including the enthalpy of the transitions.

	T_1 (°C)	ΔH_1 (J/g)	T_2 (°C)	ΔH_1 (J/g)	T_c (°C)	ΔH_c (J/g)
OXA 2,6	41	5.7	-	-	278	137.8
OXA 3,6	58	5.9	-	-	220	114.6
OXA 4,6	53	14.24	153.32	19.1	245	148.8

Determination of Peak crystallization temperatures of *i*PP, and self-assembly temperatures of nucleating agents

The information obtained in Figures 4 and 6 of the original manuscript were extracted from the differential scanning calorimetry thermograms of *i*PP samples containing various amount of NA. The experiments were performed at a heating and cooling rate of 10 °C/min between 25 °C and 220 °C. For illustration, the second heating and cooling DSC runs for the samples containing 0.1, 0.3, 0.5 and 1 wt% of **OXA 4,6** are depicted in Figure S1 (A and C). Furthermore, the melting and crystallization processed of the nucleating agent in the *i*PP melt, as observed in DSC analysis, is depicted in Figures S1 C and D. Figure S1 shows melting of the nucleating agents above the melting temperature of the *i*PP phase, however melting of the nucleating agent is found to be spread over a broad temperature range (baselines indicated by the black dotted lines). The crystallization process of **OXA 4,6** from the *i*PP melt is more sharp, and the peak values of these transitions are taken as the self-assembly temperatures depicted in Figure 4 of the manuscript. Similarly, from the second DSC cooling run, the onset temperature of crystallization and peak temperature of crystallization are extracted, which are used as data points in Figure 6.

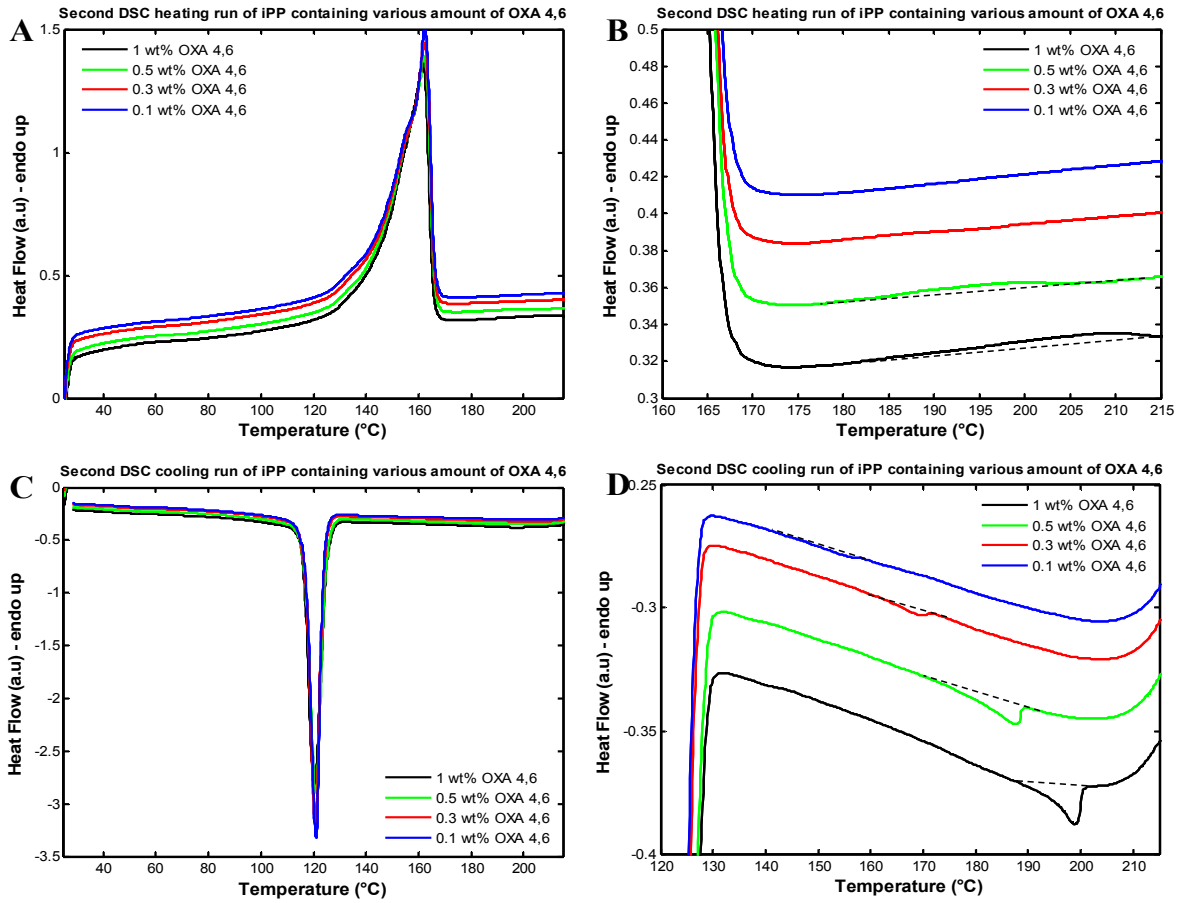

Figure S1. Figure A) depicts the second DSC heating traces showing melting of the *i*PP crystals in *blends* containing various amounts of **OXA 4,6**, whereas B) is the magnified view of Figure A showing melting of the nucleating agent above the melting temperature of the *i*PP crystals. Similarly, C) depicts the second DSC cooling traces of the same samples, and D) is the magnified view of Figure C, depicting crystallization of **OXA 4,6**, upon cooling. All DSC experiments were performed at a heating and cooling rate of 10 °C/min between 25 °C and 220 °C.

DSC thermograms of *i*PP/NA blends having very low concentrations of nucleating agent

To verify if the nucleating agents can have a negative effect on the crystallization behavior of *i*PP, for the concentrations where the nucleating agent does not crystallize upon cooling, DSC experiments were performed using 0.05 wt% of **OXA 3,6** and **OXA 4,6** in *i*PP. The second crystallization curves are compared with crystallization of the as-extruded *i*PP (thus containing 1 wt% Irganox 1010). From Figure S2, it is apparent that no negative effects on the peak crystallization temperature and enthalpy of crystallization are observed. It is likely that, under these low concentrations of NA the Irganox 1010, which is present as antioxidant in all samples, is the most dominant nucleating agent.

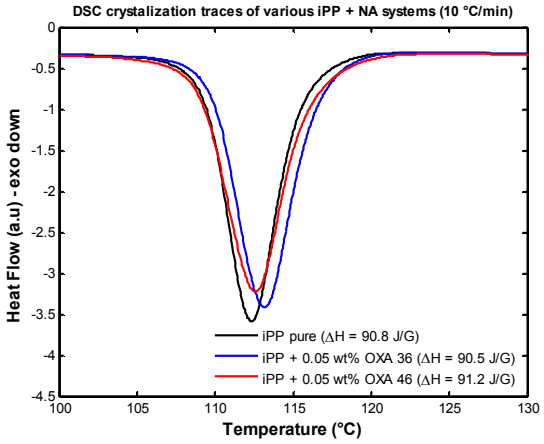

Figure S2. DSC cooling curves of as-extruded *i*PP, *i*PP containing 0.05 wt% OXA 3,6 and *iPP* containing 0.5 wt% OXA 4,6, observed during cooling from 220 °C to room temperature at a cooling rate of 10 °C/min."

Wide angle diffraction patterns and crystallinity of the nucleated *i*PP samples

Wide angle X-ray diffraction experiments have been performed on *i*PP blends containing 0.5 wt% of **OXA 2,6**, **OXA 3,6** and **OXA 4,6** after crystallization under quiescent conditions. Samples were allowed to crystallize during cooling at a rate of 10 °C/min from 200 °C to room temperature. In general, it is observed that the *i*PP without nucleating agent and in the blends that contain **OXA 2,6** and **OXA 3,6**, crystallizes into the α-phase (Figure S3). However, in the blend containing **OXA 4,6**, the presence of the (300) reflection corresponding to the beta crystal phase is detected (Figure S3). Peak fitting (Lorentzian peak shape) of the WAXD pattern of the sample containing **OXA 4,6** suggests an overall crystallinity of 55%, where approximately 45% of the crystalline fraction consists of beta-phase crystals. This value corresponds well with the crystallinity calculated from the enthalpy of the melting transition as observed in DSC analysis, which is found to be 50% (ΔH_m = 103 J/g for iPP containing 0.5 wt% **OXA 4,6**, taking the heat of fusion of 100% crystalline *i*PP to be of 207 J/G).[1]

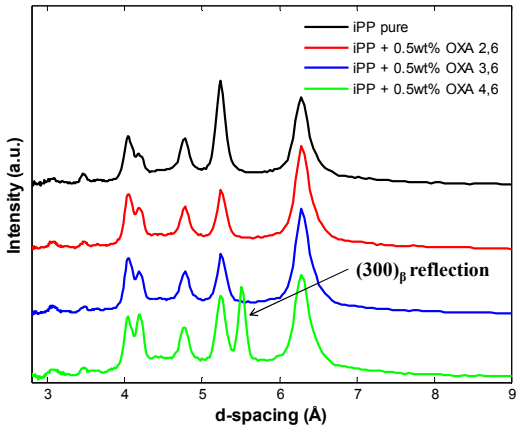

Figure S3. WAXD patterns of *i*PP/NA blends containing 0.5 wt% **OXA 2,6**, **OXA 3,6**, and **OXA 4,6**, and pure *i*PP. The samples were crystallized during continuous cooling from 200 °C at a rate of 10 °C/min to room temperature, prior to WAXD analysis.

Effect of cooling rate on the self-assembly of nucleating agent and its influence on the crystallization of *i*PP

To demonstrate that an increased cooling rate enhances crystallization of nucleating agent with increased S/V ratio, retrospectively influencing the crystallization of iPP, comparative experiments of pure *i*PP sample having no oxalamide are performed. To avoid oxidation, the pure *i*PP was mixed with 1 wt% of Irganox 1010. The observations are that the Irganox 1010 compound itself acts as a mild nucleating agent, because the peak crystallization temperature shifts to 111-112 °C. To recall, for pure iPP powder having no antioxidant, for the same crystallization conditions the peak crystallization temperature at 109 °C is observed. The minor shift in the crystallization temperature may be also attributed to the inclusion of impurities during extrusion. Independent of the nucleation induced by the impurities inclusion during extrusion and/or the addition of Irganox 1010, the crystallization temperature of *i*PP remains independent of the cooling rate (Figure S4, left). In contrast, the samples having 0.5 wt% of **OXA 4,6**, (Figure 8 of the manuscript) or **OXA 3,6** (Figure S4, right) show a shift in peak crystallization temperature. The data confirms that an increased cooling rate promotes self-assembly of the nucleating agents into aggregates having larger S/V ratio, retrospectively enhancing the number of heterogeneous nucleation sites for *i*PP.

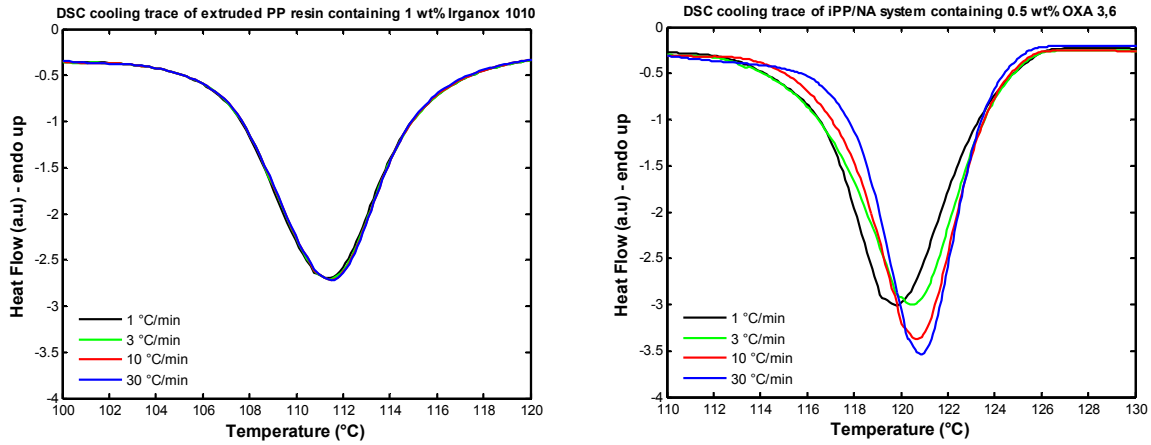

Figure S4. DSC crystallization curves observed during cooling at a rate of 10 °C/min from 180 °C to room temperature (25 °C) for the *i*PP resin with 1 wt% anti-oxidant (Irganox 1010) after extrusion (left), and the *i*PP resin containing an additional 0.5 wt% **OXA 3,6** (right). Prior to crystallization during cooling at a rate of 10 °C/min, the samples were cooled from 220 °C to 180 °C at various rates, being 1, 3, 10 and 30 °C/min.

Increase in complex viscosity during crystallization in the rheometer for the *i*PP blend containing 0.5 wt% OXA 4,6.

Figure S5 shows the increase in complex viscosity for the *i*PP sample containing 0.5 wt% of **OXA 4,6**, as observed during cooling at a rate of 5 °C. The onset of crystallization of *i*PP is detected at 130 °C when no shear pulse is applied during cooling. This corresponds to an increase of 7 °C compared to the pure *i*PP, as shown in Figure 12 of the manuscript. When a shear pulse is applied during cooling at 170 °C (60 s^{-1}, 3 s), the onset of crystallization of *i*PP shifts further to 136 °C. To reflect, the *i*PP in the blend containing 0.5 wt% **OXA 3,6** exhibited an onset of crystallization at 132 °C under the same conditions. This indicates that **OXA 4,6** is a slightly better nucleating agent that **OXA 3,6**, under these conditions.

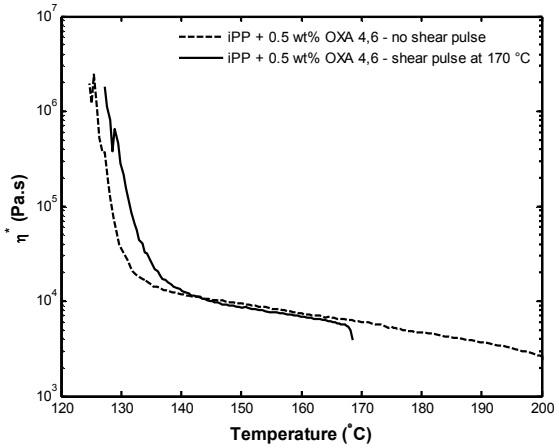

Figure S5. Change in complex viscosity of *i*PP containing 0.5 wt% **OXA 4,6** observed during cooling and crystallization in the rheometer. The onset of crystallization is defined as the intersection of the tangential lines of the complex viscosity before and during the crystallization process. *N.b.* the shear pulse in this protocol (60 s^{-1} for 3 s) is applied at 170 °C.

---

(1) B. Wunderlich, *Thermal Analysis*, Academic Press, **1990**, pp. 417-431